


AUTHOR QUERY FORM

	<p>Journal: Appl. Phys. Lett.</p> <p>Article Number: 003631APL</p>	<p>Please provide your responses and any corrections by annotating this PDF and uploading it according to the instructions provided in the proof notification email.</p>
---	--	--

Dear Author,

Below are the queries associated with your article; please answer all of these queries before sending the proof back to AIP. Please indicate the following:

Figures that are to appear as color online only (i.e., Figs. 1, 2, 3) _____ (this is a free service).
 Figures that are to appear as color online and color in print _____ (a fee of \$325 per figure will apply).

Article checklist: In order to ensure greater accuracy, please check the following and make all necessary corrections before returning your proof.

1. Is the title of your article accurate and spelled correctly?
2. Please check affiliations including spelling, completeness, and correct linking to authors.
3. Did you remember to include acknowledgment of funding, if required, and is it accurate?

Location in article	Query / Remark: click on the Q link to navigate to the appropriate spot in the proof. There, insert your comments as a PDF annotation.
AQ1	Please check that the author names are in the proper order and spelled correctly. Also, please ensure that each author's given and surnames have been correctly identified (given names are highlighted in red and surnames appear in blue).
AQ2	Sections headings are not allowed in APL. Therefore, all headings have been deleted throughout the article.
AQ3	Fig. 6 was not cited in the text. We have inserted a citation in the sentence beginning "In this work..." Please check and reposition if necessary.
AQ4	Please define CPLD at first occurrence.
AQ5	Please provide Report Number for Ref. 4.
AQ6	If e-print Ref. 41 has subsequently been published elsewhere, please provide updated reference information (journal title, volume number, page number, and year).
AQ7	Please check the presentation of Ref. 50.
AQ8	We were unable to locate a digital object identifier (doi) for Ref(s). 2,3,15,21,22,43, and 44. Please verify and correct author names and journal details (journal title, volume number, page number, and year) as needed and provide the doi. If a doi is not available, no other information is needed from you. For additional information on doi's, please select this link: http://www.doi.org/ .

Thank you for your assistance.

1 Random numbers from vacuum fluctuations

Yicheng Shi,^{1,2} Brenda Chng,² and Christian Kurtsiefer^{1,2,a)}

¹Department of Physics, National University of Singapore, 2 Science Drive 3, Singapore 117542

²Center for Quantum Technologies, National University of Singapore, 3 Science Drive 2, Singapore 117543

(Received 26 February 2016; accepted 15 July 2016; published online xx xx xxxx)

We implement a quantum random number generator based on a balanced homodyne measurement of vacuum fluctuations of the electromagnetic field. The digitized signal is directly processed with a fast randomness extraction scheme based on a linear feedback shift register. The random bit stream is continuously read in a computer at a rate of about 480 Mbit/s and passes an extended test suite for random numbers. *Published by AIP Publishing.* [<http://dx.doi.org/10.1063/1.4959887>]

Various cryptographic schemes, classical or quantum, require high quality and trusted random numbers for key generation and other aspects of the protocols. In order to keep up with data rates in modern communication schemes, these random numbers need to be generated at a high rate.¹ Equally, large amounts of random numbers are at the core of Monte Carlo simulations.² Algorithmically generated pseudo-random numbers are available at very high rates but are deterministic by definition and therefore unsuitable for cryptographic purposes. For applications that require unpredictable random numbers, hardware random number generators have been used in the past³ and more recently.⁴ These involve measuring noisy physical processes and conversion of the outcome into random numbers. Since it is either practically (e.g., for thermal noise sources) or fundamentally impossible to predict the outcome of such measurements, these physically generated random numbers are considered “truly” random.

Quantum random number generators (QRNGs) belong to a class of hardware random number generators where the source of randomness is the fundamentally unpredictable outcome of quantum measurements. Early QRNGs were based on observing the decay statistics of radioactive nuclei.^{5,6} More recently, similar QRNGs based on Poisson statistics in optical photon detection have been reported.^{7–13} Different schemes use the randomness of a single photon scattered by a beam splitter into either of two output ports.^{14,15} As the reflection/transmission of the photon is intrinsically random due to the quantum nature of the process, the unpredictability of the generated numbers is ensured.¹⁶ Other implementations of QRNGs measure the amplified spontaneous emission,¹⁷ the vacuum fluctuations of the electromagnetic field,^{18–20} or the intensity^{21,22} and phase noise of different light sources.^{23–30}

In this paper, we report on a QRNG based on measuring vacuum fluctuations of a light field as the source of randomness.^{18–20} Such measurements have a very high bandwidth compared to schemes based on photon counting,^{7–13} and have a much simpler optical setup compared to phase noise measurements.^{23–30} Coupled with an efficient randomness extractor, we obtain an unbiased, uncorrelated stream of random bits at a high rate.

Figure 1 schematically shows the setup of our QRNG. A continuous wave laser (wavelength 780 nm) is used as the local oscillator (LO) for the vacuum fluctuations entering the beam splitter at the empty port. The output of the beam splitter is directed onto two photodiodes, and the photocurrent difference is processed further. This setup is known as a balanced homodyne detector^{31,32} and maps the electrical field in the second mode entering the beam splitter to the photocurrent difference $i_1 - i_2$. Here, the second input port is empty, so the homodyne measurement is probing the vacuum state of the electromagnetic field. This field fluctuates³³ and is used as the source of randomness. As the vacuum field is independent of external physical quantities, it cannot be tampered with. Since the optical power impinging on the two photodiodes is balanced, any power fluctuation in the local oscillator will be simultaneously detected, and therefore cancel in the photocurrent difference.^{32,34} In an alternative view, the laser beam can be seen as generating photocurrents i_1 and i_2 with a shot noise power proportional to the average optical power. The shot noise currents from the diodes add up as they are uncorrelated, while amplitude fluctuations in the laser intensity (referred to as classical noise) do not affect the photocurrent difference.

The power of the two output ports is balanced by rotating the laser diode in front of a polarizing beam splitter

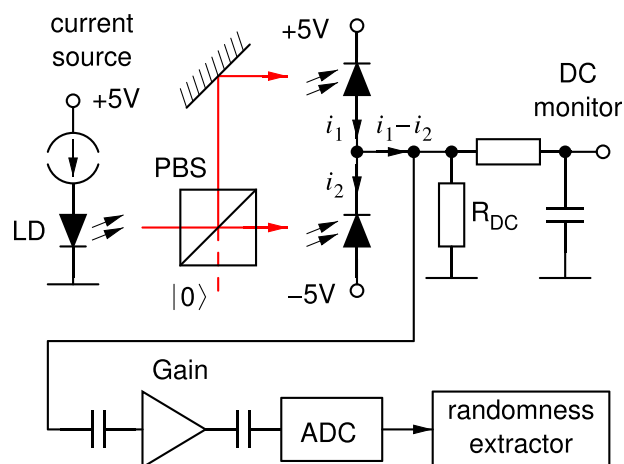


FIG. 1. Schematic of the quantum random number generator. A polarizing beam splitter (PBS) distributes light from a 780 nm laser equally onto two photodiodes, generating photocurrents i_1 and i_2 . The current difference $i_1 - i_2$ is amplified, digitized, and processed to generate random numbers.

^{a)}christian.kurtsiefer@gmail.com

78 (PBS). Light leaving the PBS is detected by a pair of reverse
 79 biased silicon pin photodiodes (Hamamatsu S5972) con-
 80 nected in series to perform the current subtraction. The bal-
 81 ancing of photocurrents is monitored by observing the
 82 voltage drop across a resistor R_{DC} providing a DC path from
 83 the common node to ground. We achieve a 50 dB rejection
 84 ratio of the classical noise from the laser intensity fluctua-
 85 tions by careful balancing. The fluctuations $\Delta(i_1 - i_2)$ above
 86 20 MHz are amplified by a transimpedance amplifier
 87 (Analog Devices AD8015) followed by two wideband RF
 88 gain blocks (Mini Circuits MAR-6). The entire amplifier
 89 chain has a calculated effective transimpedance of $R_{\text{eff}} \approx$
 90 $540 \pm 118 \text{ k}\Omega$.

91 To ensure that the fluctuations at the amplifier output are
 92 dominated by quantum noise, the spectral power density is
 93 measured (see Fig. 2). With an optical power of 3.1 mW
 94 received by each photodiode corresponding to an average
 95 photocurrent $I = 1.7 \text{ mA}$, we observe a noise power of $P =$
 96 -53.5 dBm (at 75 MHz) in a bandwidth of $B = 1 \text{ kHz}$. This
 97 is about 1.5 dB lower than the theoretically expected shot
 98 noise value (dashed trace)

$$P = \frac{4eIBR_{\text{eff}}^2}{Z} \approx -52 \text{ dBm}, \quad (1)$$

99 where e is the electron charge and $Z = 50 \Omega$ the load imped-
 100 ance.³⁵ The difference is compatible with uncertainties in
 101 determining the transimpedance of the amplifier. The mea-
 102 sured total noise has a relatively flat power density in the
 103 range of 20–120 MHz, with high pass filters in the circuit
 104 suppressing low frequency fluctuations. The high end of the
 105 pass band is defined by the cutoff frequency of the amplifier.
 106 To illustrate the effectiveness of removing classical noise in
 107 the photocurrents, the spectral power density of the photo-
 108 current generated from a single diode is also shown. Strong
 109 spectral peaks at various radio frequencies appear to enter
 110 the system probably via the laser diode current. For comple-
 111 teness, the spectral power density of the electronic noise
 112 is recorded without any optical input and found to be at least

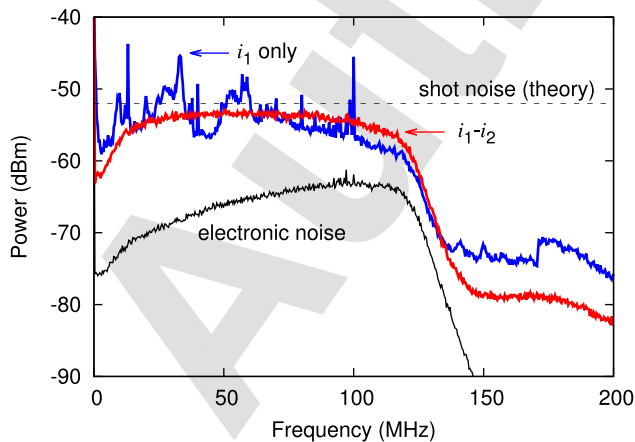


FIG. 2. Amplified noise levels measured into a resolution bandwidth $B = 1 \text{ kHz}$. The total noise is measured from the photocurrent difference $i_1 - i_2$ with equal optical power impinging on both photodiodes and approaches the theoretical shot noise level of -52 dBm (dashed trace) given by (1). The current i_1 of a single photodiode reveals colored classical noise. The electronic noise is measured without any optical input.

10 dB below the total noise level, i.e., the total noise is domi-
 113 nated by quantum fluctuations. 114

The amplified total noise is digitized into signed 16 bit
 115 words x_i at a sampling rate of 60 MHz with an analog to digi-
 116 tal converter (ADC, Analog Devices AD9269-65). The sam-
 117 pling rate is lower than the cut-off frequency of the noise
 118 signal to avoid temporal correlation between samples. As
 119 shown in Fig. 3, the normalized autocorrelation 120

$$A(d) = \langle x_i x_{i+d} \rangle_n / \langle x_i^2 \rangle_n, \quad (2)$$

evaluated over $n = 10^9$ samples shows that the absolute 121
 value of the autocorrelation $|A(d)|$ for non-zero delay ($d > 0$) 122
 is below 1.2×10^{-3} , which is slightly smaller than what has 123
 been observed in other experiments.^{23,36,37} The residual cor- 124
 relation above the 2σ confidence level for $d \lesssim 60$ is a conse- 125
 quence of the finite bandwidth of the signal, as stated by the 126
 Wiener-Khinchin theorem. 127

The total noise measured before the ADC contains both 128
 quantum and electronic noise. To determine how much ran- 129
 domness from the non-classical origin can be safely 130
 extracted, it is necessary to estimate the entropy $H(X_q)$ con- 131
 tributed by the quantum process. 132

Therefore, we assume that the measured total noise sig- 133
 nal $X_t = X_q + X_e$ is the sum of independent random variables 134
 X_q for the quantum noise, and X_e for the electronic noise 135
 which includes the photodetector, amplifier, and digitizer 136
 noise.^{22,37} All three variables X_q , X_e , and X_t are assumed 137
 to have discrete values between -2^{15} and $2^{15} - 1$. We take the 138
 worst case scenario that an adversary has full knowledge of 139
 the electronic noise, i.e., is able to predict the exact outcome 140
 of X_e at any moment. In this case, the amount of quantum- 141
 based randomness in the acquired total noise signal is quanti- 142
 fied by the conditional entropy $H(X_t|X_e)$, i.e., the entropy in 143
 the total signal, given full knowledge of the electronic noise 144
 X_e . As the variables are assumed to be additive and independ- 145
 ent, the conditional entropy is $H(X_t|X_e) = H(X_q + X_e|X_e)$ 146
 $= H(X_q|X_e) = H(X_q)$. 147

The variance of the total noise, σ_t^2 , is given by the sum 148
 of the variances σ_q^2 for the quantum noise, and σ_e^2 for the 149
 electronic noise. Over 10^9 samples, we find $\sigma_t = 4504.41$ 150
 and $\sigma_e = 1481.8$, measured with the laser switched off (see 151

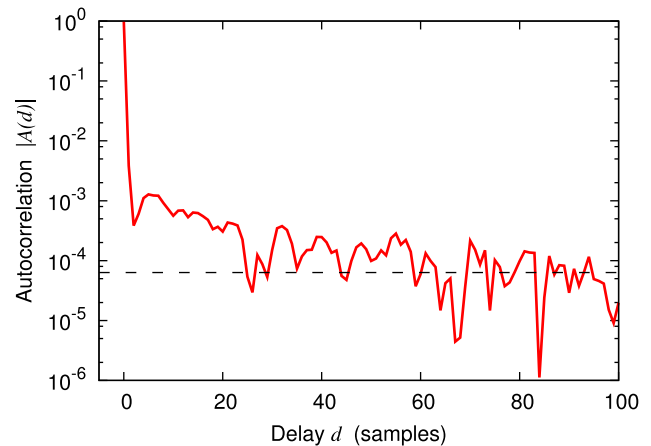


FIG. 3. Autocorrelation of the total noise signal sampled at 60 MHz, computed over 10^9 samples (solid line), compared with the 2σ confidence level (dashed line).

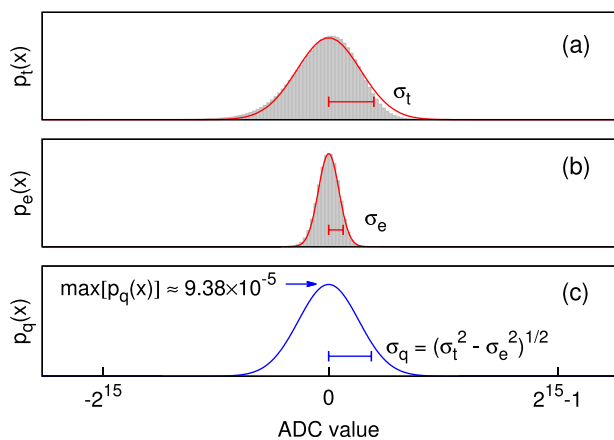


FIG. 4. Probability distribution of the measured total noise with variance σ_t^2 (a), electronic noise with variance σ_e^2 (b), and the estimated quantum noise with variance σ_q^2 (c). The filled areas in (a), (b) show the actual measurements over 10^9 samples, the solid lines fit to Gaussian distributions.

152 Fig. 4). Note that for the total noise, the observed distribution
 153 is slightly skewed compared to a Gaussian distribution [solid
 154 line in Fig. 4(a)], possibly due to a distortion in the digitizer.
 155 Assuming the quantum noise X_q has a Gaussian distribu-
 156 tion,³³ we would assign a variance $\sigma_q^2 = \sigma_t^2 - \sigma_e^2 \approx 4253.7^2$.
 157 To estimate the entropy for a Gaussian distribution, we use
 158 the Shannon entropy

$$H_S(X_q) = \sum_{x=-2^{15}}^{2^{15}-1} -p_q(x) \log_2 p_q(x), \quad (3)$$

159 where $p_q(x)$ is the probability distribution of the quantum
 160 noise X_q . Since $\sigma_q \gg 1$, $H_S(X_q)$ can be well approximated
 161 by

$$\int_{-\infty}^{+\infty} -f(x) \log_2 f(x) dx = \log_2(\sqrt{2\pi e} \sigma_q), \quad (4)$$

162 where $f(x)$ is a Gaussian probability density function with
 163 variance σ_q^2 and e the base of the natural logarithm.³⁸ This
 164 yields 14.1 bits of entropy per 16 bit sample. We also evalu-
 165 ate the min-entropy of this distribution

$$H_\infty(X_q) = -\log_2(\max[p_q(x)]) \approx \log_2(\sqrt{2\pi} \sigma_q), \quad (5)$$

166 where $\max[p_q(x)]$ is the maximum value of the probability
 167 distribution of X_q . This yields a min-entropy of 13.4 bits per
 168 16 bit sample.

169 The Shannon entropy $H_S(X_q)$ serves as an upper bound
 170 of extractable randomness, while the min-entropy sets a
 171 lower bound, i.e., the least amount of randomness possessed
 172 by each sample. An alternative estimation of the entropy in
 173 X_q assumes that electronic noise is not only known to a third
 174 party but also could be tampered with.^{19,36,39}

175 In many applications, random numbers are required to
 176 be not only unpredictable but also uniformly distributed. As
 177 such, the raw ADC output cannot be directly used.
 178 Randomness extractors convert non-uniformly distributed
 179 raw data into a uniformly distributed binary stream without
 180 correlations.⁴⁰ Although there is no deterministic universal

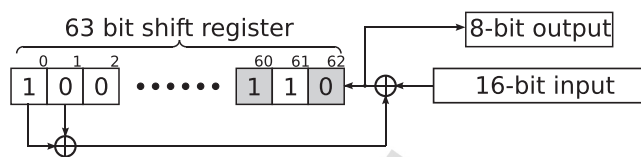


FIG. 5. Schematic of a LFSR-based randomness extractor. Eight bits (from the shaded positions) are extracted for every 16 bits of input.

181 randomness extractor,⁴⁰ various practical implementations
 182 have been reported. Examples are Trevisan's extractor, a
 183 Toeplitz hashing extractor,³⁷ random matrix multiplica-
 184 tions,^{22,41} or a family of secure hashing algorithms (SHA).¹⁸

185 In this work, we use a randomness extractor based on a
 186 Linear Feedback Shift Register (LFSR) as shown in Figs. 5
 187 and 6, equivalent to a cyclic redundancy check (CRC).⁴² The
 188 LFSRs are well known for generating long pseudo-random
 189 streams with little computational resources and are in wide-
 190 spread use in communication applications for spectrum
 191 whitening.⁴³⁻⁴⁷

192 We use a maximum length LFSR with 63 cells and a
 193 two-element feedback path. Its state at any time t is a row
 194 vector S_t of 63 bits, with a recursion relation

$$S_{t+1} = S_t M + R_t$$

$$= (s_0, s_1, s_2, \dots, s_{62}) \begin{pmatrix} 0 & 0 & \dots & 0 & 1 \\ 1 & 0 & \dots & 0 & 1 \\ 0 & 1 & \dots & 0 & 0 \\ \vdots & \vdots & \ddots & \vdots & \vdots \\ 0 & 0 & \dots & 1 & 0 \end{pmatrix} + (0, 0, 0, \dots, 0, r_t)$$

$$= (s_1, s_2, s_3, \dots, s_{62}, s_0 + s_1 + r_t), \quad (6)$$

195 where an elementary addition represents a binary **xor**, and a
 196 multiplication a binary **and** operation.

197 The 63×63 matrix M represents the shift and feedback
 198 operation on the LFSR state. The addition of row vector R_t
 199 describes the injection of one raw random bit r_t into S_t . After
 200 n cycles, the LFSR state becomes

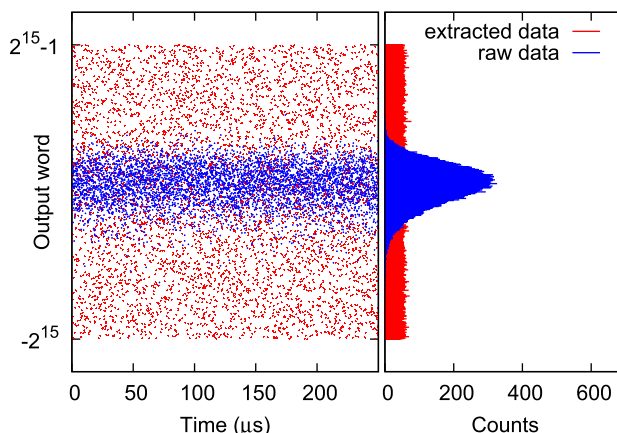


FIG. 6. Distribution of random data before (blue) and after (red) the randomness extractor, shown in time domain (left) and histogram (right).

$$S_{t+n} = S_t M^n + \underbrace{R_t M^{n-1} + \dots + R_{t+n-1}}_A. \quad (7)$$

201 Row vector A can be expressed as a matrix product

$$A = (r_t, r_{t+1}, \dots, r_{t+n-1})T, \quad (8)$$

202 with

$$T = \begin{pmatrix} S'M^{n-1} \\ S'M^{n-2} \\ \vdots \\ S'I \end{pmatrix}, \quad S' = (0, 0, \dots, 0, 1). \quad (9)$$

203 Matrix T in (9) is a 63×63 Toeplitz matrix with rows gener-
204 ated from a LFSR sequence (6) with $R_t=0$ and initial state
205 $S_t = S'$. It was shown that multiplying an input stream by
206 such a Toeplitz matrix can be used as a hashing function that
207 generates an almost-uniform output.⁴³

208 In our setup, we serially inject the 16 bits from each ADC
209 output word into the LFSR but extract only 8 bits s_i provided
210 by stream S_i (at positions 62, 60, ..., 48 after the injection) in
211 a parallelized topology. This is equivalent to a privacy ampli-
212 fication process⁴⁸ and ensures that no residual correlations due
213 to the non-uniform input distribution or any classical noise
214 that may be known to an adversary are present in the output
215 stream, because the extraction ratio of 50% is lower than the
216 $13.4/16 \approx 84\%$ allowed by the **min entropy** (5).

217 A merit of this extractor is its low complexity. Unlike
218 many other secure hashing algorithms, it can be easily imple-
219 mented either in high speed or low power technology.
220 Therefore, the extraction process does not limit the random
221 number generation rate. This scheme can be parallelized
222 using 126 register cells, capable of receiving up to 63
223 injected raw bits per clock cycle while still following the
224 extractor equation (6). With a **CPLD** operating at a clock fre-
225 quency of 400 MHz, this algorithm would be able to process
226 up to 25×10^9 raw input bits per second.

227 To evaluate the quality of the extracted random numbers,
228 we apply two suites of randomness tests: the statistical test
229 suite from NIST⁴⁹ and the “Die-harder” randomness test bat-
230 tery.⁵⁰ The output of our RNG passed both tests consistently
231 when evaluated over a sample of 400 Gigabit in the sense that
232 occasional weak outcomes of some tests do not repeat.

233 Our implementation has an output rate of about 480
234 Mbit/s of uniformly distributed random bits, with the digi-
235 tizer unit sampling at 60 MHz and randomness extraction
236 ratio of 50%; this is limited by the speed of the data trans-
237 mission protocol (USB2.0). While significantly higher gener-
238 ation rates have been reported recently,^{17,23,25} our design in
239 comparison is simpler both in hard- and software implemen-
240 tation. With moderate effort, our random number generation
241 rate can be greatly increased by extending the bandwidth of
242 the photodiodes, amplifiers, and digitizer devices, while
243 maintaining the relatively simple randomness extraction
244 mechanism. Practically, the resolution-bandwidth product of
245 the ADC limits the random bit generation rate.

246 In summary, we demonstrated a random number genera-
247 tion scheme by measuring the vacuum fluctuations of the elec-
248 tromagnetic field. By estimating the amount of usable entropy

from quantum noise and using an efficient randomness extrac- 249
tor based on a linear feedback shift register, we can generate 250
uniformly distributed random numbers at a high rate from a 251
fundamentally unpredictable quantum measurement. 252

We acknowledge the support of this work by the National 254
Research Foundation (partly under Grant No. NRF-CRP12- 255
2013-03) & Ministry of Education in Singapore, partly 256
through the Academic Research Fund MOE2012-T3-1-009. 257

¹N. Gisin, G. Ribordy, W. Tittel, and H. Zbinden, *Rev. Mod. Phys.* **74**, 145 259
(2002). 260

²N. Metropolis, *Los Alamos Sci.* **15**, 125 (1987). 261

³E. Galton, *Nature* **42**, 1314 (1890). 262

⁴B. Jun and P. Kocher, “The intel random number generator,” Technical 263
Report No. **■** (Cryptography Research Inc., 1999). 264

⁵M. Gude, *Frequenz* **39**, 187 (1985). 265

⁶A. Figotin, I. Vitebskiy, V. Popovich, G. Stetsenko, S. Molchanov, A. 266
Gordon, J. Quinn, and N. Stavrakas, “Random number generator based on 267
the spontaneous alpha-decay,” U.S. patent 6,745,217 (2004). 268

⁷M. Stipevcic and B. M. Rogina, *Rev. Sci. Instrum.* **78**, 045104 (2007). 269

⁸M. A. Wayne, E. R. Jeffrey, G. M. Akselrod, and P. G. Kwiat, *J. Mod. 270
Opt.* **56**, 516 (2009). 271

⁹M. Fürst, H. Weier, S. Nauerth, D. G. Marangon, C. Kurtsiefer, and H. 272
Weinfurter, *Opt. Express* **18**, 13029 (2010). 273

¹⁰M. A. Wayne and P. G. Kwiat, *Opt. Express* **18**, 9351 (2010). 274

¹¹M. Wahl, M. Leifgen, M. Berlin, T. Rohlicke, H.-J. Rahn, and O. Benson, 275
Appl. Phys. Lett. **98**, 171105 (2011). 276

¹²Y.-Q. Nie, H.-F. Zhang, Z. Zhang, J. Wang, X. Ma, J. Zhang, and J.-W. 277
Pan, *Appl. Phys. Lett.* **104**, 051110 (2014). 278

¹³M. Ren, E. Wu, Y. Liang, Y. Jian, G. Wu, and H. Zeng, *Phys. Rev. A* **83**, 279
023820 (2011). 280

¹⁴T. Jennewein, U. Achleitner, G. Weihs, H. Weinfurter, and A. Zeilinger, 281
Rev. Sci. Instrum. **71**, 1675 (2000). 282

¹⁵A. Stefanov, N. Gisin, O. Guinnard, L. Guinnard, and H. Zbinden, *J. Mod. 283
Opt.* **47**, 595 (2000). 284

¹⁶D. Frauchiger and R. Renner, *Proc. SPIE* **8899**, 88990S (2013). 285

¹⁷C. R. S. Williams, J. C. Salevan, X. Li, R. Roy, and T. E. Murphy, *Opt. 286
Express* **18**, 23584 (2010). 287

¹⁸C. Gabriel, C. Wittmann, D. Sych, R. Dong, W. Maurer, U. L. Andersen, 288
C. Marquardt, and G. Leuchs, *Nat. Photonics* **4**, 711–715 (2010). 289

¹⁹T. Symul, S. M. Assad, and P. K. Lam, *Appl. Phys. Lett.* **98**, 231103 290
(2011). 291

²⁰Y. Shen, L. Tian, and H. Zou, *Phys. Rev. A* **81**, 063814 (2010). 292

²¹I. Kanter, Y. Aviad, I. Reidler, E. Cohen, and M. Rosenbluh, *Nat. 293
Photonics* **4**, 5861 (2009). 294

²²B. Sanguinetti, A. Martin, H. Zbinden, and N. Gisin, *Phys. Rev. X* **4**, 295
031056 (2014). 296

²³Y.-Q. Nie, L. Huang, Y. Liu, F. Payne, J. Zhang, and J.-W. Pan, *Rev. Sci. 297
Instrum.* **86**, 063105 (2015). 298

²⁴B. Qi, Y.-M. Chi, H.-K. Lo, and L. Qian, *Opt. Lett.* **35**, 312 (2010). 299

²⁵F. Xu, B. Qi, X. Ma, H. Xu, H. Zheng, and H.-K. Lo, *Opt. Express* **20**, 300
12366 (2012). 301

²⁶C. Abellán, W. Amaya, M. Jofre, M. Curty, A. Acn, J. Capmany, V. 302
Pruneri, and M. W. Mitchell, *Opt. Express* **22**, 1645 (2014). 303

²⁷C. Abellán, W. Amaya, D. Mitrani, V. Pruneri, and M. W. Mitchell, *Phys. 304
Rev. Lett.* **115**, 250403 (2015). 305

²⁸Z. L. Yuan, M. Lucamarini, J. F. Dynes, B. Frhlich, A. Plews, and A. J. 306
Shields, *Appl. Phys. Lett.* **104**, 261112 (2014). 307

²⁹H. Zhou, X. Yuan, and X. Ma, *Phys. Rev. A* **91**, 062316 (2015). 308

³⁰M. Jofre, M. Curty, F. Steinlechner, G. Anzolin, J. P. Torres, M. W. 309
Mitchell, and V. Pruneri, *Opt. Express* **19**, 20665 (2011). 310

³¹E. Jakeman, C. Oliver, and E. Pike, *Adv. Phys.* **24**, 349 (1975). 311

³²H. P. Yuen and V. W. Chan, *Opt. Lett.* **8**, 177 (1983). 312

³³R. J. Glauber, *Phys. Rev.* **131**, 2766 (1963). 313

³⁴B. L. Schumaker, *Opt. Lett.* **9**, 189 (1984). 314

³⁵W. Schottky, *Ann. Phys.* **362**, 541–567 (1918). 315

³⁶M. W. Mitchell, C. Abellán, and W. Amaya, *Phys. Rev. A* **91**, 012314 (2015). 316

³⁷X. Ma, F. Xu, H. Xu, X. Tan, B. Qi, and H.-K. Lo, *Phys. Rev. A* **87**, 317
062327 (2013). 318

³⁸One can show that $|H(X_q) - H'(X_q)| < \log_2(\sqrt{2\pi}\sigma_q)/(\sqrt{2\pi}\sigma_q) \approx 0.0013$ 319
bit for $\sigma_q = 4108$. 320

- 321 ³⁹J. Y. Haw, S. M. Assad, A. M. Lance, N. H. Y. Ng, V. Sharma, P. K. Lam,
322 and T. Symul, *Phys. Rev. Appl.* **3**, 054004 (2015). 333
- 323 ⁴⁰M. Santha and U. V. Vazirani, *J. Comput. Syst. Sci.* **33**, 75 (1986). 334
- 324 ⁴¹D. Frauchiger, R. Renner, and M. Troyer, e-print arXiv:1311.4547 [quant-
325 ph]. 335
- AQ6 ⁴²W. W. Peterson and D. T. Brown, *Proc. IRE* **49**, 228 (1961). 336
- 326 ⁴³H. Krawczyk, *Adv. Cryptol.* **94**, 129139 (1994). 337
- 327 ⁴⁴E. Barkan, E. Biham, and N. Keller, *J. Cryptol.* **21**, 392429 (2007). 338
- 328 ⁴⁵T. E. Tkacik, in *Cryptographic Hardware and Embedded Systems-CHES*
329 *2002*, Lecture Notes in Computer Science Vol. 2523, edited by B. S. 339
- 330 Kaliski, C. K. Koç, and C. Paar (Springer, Berlin, Heidelberg, 2003), pp. 340
- 331 450–453. 341
- 332 ⁴⁶S. Wells and D. Ward, “Random number generator with entropy accumu-
333 lation,” U.S. patent 6,687,721 (2004). 334
- ⁴⁷K. Tsoi, K. Leung, and P. Leong, *IET Comput. Digital Tech.* **1**, 349 (2007). 335
- ⁴⁸C. H. Bennett, G. Brassard, C. Crepeau, and U. M. Maurer, *IEEE Trans.*
336 *Inf. Theory* **41**, 1915 (1995). 337
- ⁴⁹A. Rukhin, J. Soto, J. Nechvatal, M. Smid, E. Barker, S. Leigh, M.
338 Levenson, M. Vangel, D. Banks, A. Heckert, J. Dray, and S. Vo, *A*
339 *Statistical Test Suite for Random and Pseudorandom Number Generators*
340 *for Cryptographic Applications* (National Institute of Standards and
341 Technology, 2010). 342
- ⁵⁰D. B. Robert, G. Brown, and D. Eddelbuettel, “Dieharder: A random num-
343 ber test suite,” (2004). 344